The dynamics of human cognition: increasing global integration coupled with decreasing segregation found using intracortical EEG

Josephine Cruzat[1], Gustavo Deco[1,2], Adrià Tauste[1,3], Alessandro Principe[3], Marco Calabria[1], Albert Costa[1,2], Morten L. Kringelbach[4,5,6] & Rodrigo Rocamora[3]

[1] Center for Brain and Cognition, Department of Information and Communication Technologies, Universitat Pompeu Fabra, Barcelona, Spain

[2] Institució Catalana de la Recerca i Estudis Avançats (ICREA), Barcelona, Spain

[3] Epilepsy Unit, Department of Neurology. IMIM Hospital del Mar, Universitat Pompeu Fabra, Barcelona, Spain.

[4] Department of Psychiatry, University of Oxford, Oxford, UK

[5] Center for Music in the Brain (MIB), Department of Clinical Medicine, Aarhus University, DK

[6] Institut d'études avancées de Paris, France

Corresponding author: Josephine Cruzat, Universitat Pompeu Fabra, C/ Roc Boronat 138, 08018 Barcelona, Spain. josephine.cruzat@upf.edu

Conflict of interest: The authors declare to have no conflict of interest.

Running Title: Integration and segregation underlying cognitive processing

Keywords: Segregation; Integration; Cognition; iEEG; SEEG.

Summary

Cognitive processing requires the ability to flexibly adjust and integrate information across large brain networks. More information is needed on how brain networks dynamically reorganize to allow such broad communication across many different brain regions in order to integrate the necessary information. Here, we use intracranial EEG to record neural activity from 12 epileptic patients while they perform a cognitive task in order to study how the broadness of communication changes across the underlying network spanning many different brain regions. The broadness of communication is characterized by functional measures of integration and segregation. Across all patients, we found significant increases in integration and decreases in segregation during cognitive processing, especially in the gamma band (50-90 Hz). Accordingly, we also found significantly higher level of global synchronization and functional connectivity during the execution of the cognitive task, again particularly in the gamma band. Furthermore, we demonstrate that these modulations in the level of communication across the network were not caused by changes in the level of the underlying oscillations as reflected by the corresponding power spectra.

Introduction

Intracranial electroencephalography (iEEG) recordings from the human brain provide a unique opportunity to study cognitive functions at the microscopic level directly measuring neural activity. Beyond the high level of temporal resolution intrinsic in EEG measurements, the proximity of the recording electrodes to the neural elements allows also higher levels of spatial resolution and enhanced signal-to-noise ratio (Lachaux *et al.*, 2003; Engel *et al.*, 2005). These advantages have led to novel studies in cognitive neuroscience (Lachaux *et al.*, 2012) tackling cognitive processes such as attention (Müsch *et al.*, 2014), visual perception (Ossandón *et al.*, 2012; Bertrand *et al.*, 2014), language (Sahin *et al.*, 2009; Chan et al., 2011; Hamamé *et al.*, 2014), memory (Kucewicz *et al.*, 2014; Greenberg *et al.*, 2015, Haque *et al.*, 2015), decision making (Pérez *et al.*, 2015), emotion (Murray *et al.*, 2014; Boucher *et al.*, 2015) and consciousness (Gaillard *et al.*, 2009). However, most of this research has attempted to correlate task-performance with these measurements of neural activity to assign functions to specific local brain areas. Furthermore, most studies using iEEG have focused mainly on single-electrodes analysis, using predominantly event-related potentials (see Lachaux *et al.*, 2003 for review) or spectral analysis (see Kahana, 2006 for review).

In contrast to this regional view of brain function, growing evidence reveals that human cognition relies on the flexible integration of information widely distributed across different brain regions (Bressler and Menon, 2010; Deco *et* al., 2015). Many studies have investigated the properties of the brain networks underlying cognitive processing using many different functional brain imaging techniques such as EEG (Fallani *et al.*, 2008; Wang *et al.*, 2015), MEG (Valencia *et al.*, 2008; Palva *et al.*, 2010; Kitzbichler *et al.*, 2011) and fMRI (Bassett *et al.*, 2011; Ekman *et al.*, 2012; Kinnison *et al.*, 2012; Chai *et al.*, 2016, Wang *et al.*, 2016). Despite the diversity in tasks and techniques, these studies concur in that cognitive processing appears to increase the global integration of information across neural networks, while at the same time leads to a decrease in the modularity of those networks (Kitzbichler *et al.*, 2011; Kinnison *et al.*, 2012; Ekman *et al.*, 2012, Bola and Sabel, 2015; Vatansever *et al.*, 2015; Godwin *et al.*, 2015, Liang *et al.*, 2016). However, these consistent findings associated to human cognition have not been validated in iEEG studies.

Here, we explored how cognitive processing modulates the level of integration and segregation of information in human brain networks. More specifically, we recorded iEEG data from depth electrodes stereotactically implanted for presurgical diagnosis in 12 epileptic patients performing a picture-naming task. The iEEG electrodes used a stereoelectroencephalography (SEEG) implantation methodology and covered broad regions of the brain including cortical as well subcortical regions, so that we were able to assess the global changes at the level of a broad extended network. This allowed us to investigate the network properties of the brain underlying cognitive processing using our operationally defined concepts of segregation and integration (Deco *et* al., 2015) as global network measures of brain function.

Materials and Methods

Ethics Statement

This study was approved by The Clinical Research Ethical Committee of the Municipal Institute of Health Care (CEIC-IMAS). Following the Declaration of Helsinki, patients were informed about the procedure and they gave their written consent before the experiment.

Participants

Twelve participants (3 women; all right-handed; mean age 36.4±10.1 years-old), evaluated for presurgical diagnosis in the Epilepsy Monitoring Unit of the Hospital del Mar (Barcelona, Spain), participated in the study. All patients were stereotactically implanted with depth electrodes for invasive presurgical diagnosis using a stereotactic ROSA robotic device (Medtech, France). The location of the electrodes was established only for clinical reasons using a SEEG approach. The implantation schemas were similar between all patients given that they were all under investigation for temporal lobe epilepsy. The number of electrodes used varied among 8 to 16 for patient with 5 to 15 contacts each (diameter: 0.8 mm; contacts 2 mm long, 1.5 mm apart) (Dixi Médical, France). All patients underwent an extensive neuropsychological evaluation, and normal or corrected-to-normal vision. They were within the normal range of education having completed from primary to high academic level. Table 1 summarizes personal data, pathological information and overview of implanted electrodes for each patient. Since the study aims to study the network dynamics supporting cognitive processes under normal circumstances, patients were assessed in absence of pharmacological treatment.

Cognitive Task

In the picture-naming task, participants were asked to name 128 pictures presented in three different blocks. Pictures were black & white line drawings of familiar objects from a wide range of semantic categories selected from the Snodgrass and Vanderwart (1980) set. Each picture appeared once centrally and sequentially on the computer screen in a pseudo-random order for 2000 ms followed by a fixation cross for 1000 ms (see Figure 1). Participants were instructed to overtly name every item as fast and accurately as possible in Spanish. The task was presented using the software Sketchbook Processing 2.2.1 (Programming Software, 2001 https://processing.org/) on a laptop computer located approximately 60 cm away from the patient. The accuracy of the responses was scored manually by the experimenter. An electronic processor “Arduino; UNO” was used to connect and synchronize both hardware, the XLTEK system with the computer (MacBook Pro). The application interfaced with an Arduino board that in turn was connected to the EEG amplifier, and at each trial a signal was sent through the Arduino to the EEG.

iEEG Data Acquisition and Preprocessing

Neurophysiological responses were registered by the iEEG system from deep multichannel electrodes (DIXI Microtechniques, Besançon, France, 5–18 contacts; length, 2 mm, diameter, 0.8 mm; 1.5 mm apart) placed in both cortex and subcortical structures. On average, each patient had 13±2 electrodes implanted (range 8-16) with a total of 120 ± 13 recording contacts (range 85-127). The data were acquired continuously by the Neuroworks XLTEK system (version 6.3.0, build 636) at 32 kHz with a headbox of 128 channels recorded at a sampling frequency of 500 Hz per channel.

A bipolar montage was constituted offline to increase spatial resolution by removing any confounds from the common reference signal (Jerbi *et al.*, 2009; Lachaux *et al.*, 2003). Bipolar signals were derived by differentiating neighbouring electrode pairs of recorded and not rejected consecutive channels within the same electrode array (Gaillard *et al.*, 2009; Lachaux *et al.*, 2012; Burke *et al.*, 2013; Boucher *et al.*, 2015). The continuous iEEG data was first high-pass filtered at 1 Hz and low-pass filtered at 150 Hz. To remove common line contamination an extra notch filter was applied at 50 and 100 Hz. In order, to have specific spectral information we analyze the spatio-temporal correlations of the Band Limited Power (BLP) at a given carrier frequency. For that, the analysis at a given carrier frequency $f_{carrier}$ (we consider here $f_{carrier}$= 1 to 130 Hz in steps of 4 Hz) requires first that the iEEG signals are bandpass filtered within the narrow band [$f_{carrier}$-2, $f_{carrier}$+2 Hz] and computed the corresponding envelope of each narrowband signal using the Hilbert transform (Brookes et al., 2011; Cabral et al., 2014). The Hilbert transform yields the associated analytical signals. The analytic signal represents a narrowband signal, s(t), in the time domain as a rotating vector with an instantaneous phase, $\phi(t)$, and an instantaneous amplitude, A(t), i.e., $s(t)=A(t)\cos(\phi(t))$. The phase and the amplitude (envelope of that carrier frequency) are given by the argument and the modulus, respectively, of the complex signal z(t), given by $z(t)=s(t)+i.H[s(t)]$, where i is the imaginary unit and H[s(t)] is the Hilbert transform of s(t). We further consider only the slow components of the envelope A(t) by filtering the amplitudes again below 12 Hz (Nir *et al.* 2008). Finally, the slow component of the envelope of each brain node at a given carrier frequency was used to calculate the envelope FC.

Data Analysis

Envelope Functional Connectivity (FC)

The data was segmented into two windows around stimulus presentation: the first one spanning from -500 ms to 0 (pre-task condition) from the stimulus presentation, and the second one spanning from 0 to 500 ms (task condition) from the stimulus presentation. Each trial was identified as an error or a hit and error trials were excluded from the analysis. We defined an Envelope FC for task and pre-task segments as a matrix of Pearson's correlations of the corresponding amplitude envelopes, i.e. the slow components of the BLP of iEEG signals at a given carrier frequency between two brain areas over the whole time window for a given condition (pre-task and task).

Integration

We used the measure of *integration* introduced by Deco *et al.* (2015), defined at the network level, to characterize the level of broadness of communication between regions across the whole brain. First, we filtered the data, and then we calculated the envelope FC as explained above for both pre-task and task conditions. We define integration as the size of the largest connected component in the FC matrix. More specifically, for a given absolute threshold θ between 0 and 1 (scanning the whole range), the FC (using the criteria $|FC_{ij}| < \theta$, ie a value of 0 and 1 otherwise) can be binarized and the largest subcomponent extracted as a measure of integration. In graph-theoretical terms, subcomponents are extracted from the undirected graph defined by the binarized matrix considered as an adjacency matrix. More precisely, a subcomponent is a subgraph in which any two vertices are connected to each other by paths, and which connects to no additional vertices in the super-graph (see Deco *et al.*, 2015 for details).

Segregation

As a complement of the integration, we used a modularity measure (Rubinov and Sporns, 2011) as a measure of segregation. Following Rubinov and Sporns (2011), we define modularity as a measure that quantify the goodness of a modularity partition (Newman, 2004), i.e. a complete subdivision of the network into non overlapping modules. We consider the modularity of our envelope FC matrix. This matrix contains positive and negative weights, namely the corresponding correlation between two nodes. Our measure of modularity is given by,

$$Q^{GJA} = \frac{1}{v^{+}+v^{-}} \sum_{ij} \left[(w_{ij}^{+} - e_{ij}^{+}) - (w_{ij}^{-} - e_{ij}^{-}) \right] \delta_{M_i M_j}$$

Where the total weight, $v^{\pm} = \Sigma_{ij} w_{ij}^{\pm}$, is the sum of all positive or negative connection weights (counted twice for each connection), being $w_{ij}^{+} \in (0,1]$ the weighted connection between nodes i and j. The chance-expected within-module connection weights $e_{ij}^{\pm} = \frac{s_i^{\pm} s_j^{\pm}}{v^{\pm}}$, where the strength of node i, $s_i^{\pm} = \Sigma_j w_{ij}^{\pm}$, is the sum of positive or negative connection weights of i. The delta $\delta_{MiMj} = 1$ when i and j are in the same module and $\delta_{MiMj} = 0$ otherwise (Newman, 2006). This definition is a generalisation of the standard measure of modularity for matrices with nonnegative weights, which is given by the average difference between present within-module connection weights w_{ij}^{+} and chance-expected within-module connection weights e_{ij}^{+}. As mentioned above, here we consider both positively and negatively weighted connections (envelope FC matrix). The positively weighted connections represents correlated activation patterns and hence to reinforce the placement of positively connected pairs of nodes in the same module. On the other hand, the negatively weighted connections represent anti-correlated activation patterns and reinforcing the placement of negatively connected pairs of nodes in distinct modules.

Synchronization

We measure the global mean level of synchronization as the mean value of the Kuramoto order parameter across time. The Kuramoto order parameter is defined by following equation:

$$R(t) = \left| \sum_{k=1}^{n} e^{(i\varphi(t))} \right| / n$$

where $\phi_k(t)$ is the instantaneous phase of each narrowband signal at node k. The Kuramoto order parameter measures the global level of synchronization of the n oscillating signals. Under complete independence, the n phases are uniformly distributed and thus R is nearly zero, whereas for R=1 all phases are equal (full synchronization). We compute the global mean level of synchronization of the empirical iEEG signals at a given carrier frequency by using the Hilbert derived phases of the slow component of the Band Limited Power (BLP) signals.

Results

In the present study we exploited the good spatiotemporal resolution of intracranial electroencephalography (iEEG) recordings to investigate the reorganization of brain networks driven by a cognitive task. This technique is usually employed in pharmacologically resistant epileptic patients (Sperling, 1997; Serletis *et al.*, 2014) who require brain mapping before surgery. In addition to the invaluable clinical utility and especially for the high functional, spatial and temporal specificity, iEEG recordings in epileptic patients have been increasingly used in cognitive neuroscience (Lachaux *et al.*, 2012).

We recorded iEEG data in twelve patients while performing a picture-naming task (Figure 1A). This task was used to drive the modulation of the underlying brain networks related to the integration of task-related information. It is known that language is supported by a widespread large-scale network distributed across frontal, temporal, parietal and occipital lobes in the dominant hemisphere (Ferstl et al., 2008; Price, 2000; Chai et al., 2016). During the task patients had to overtly name each picture as fast as they could in Spanish (see Materials and Methods). The picture naming accuracy was high (85.3 ± 11.0%) (Figure 1B). All channels recording from grey matter and subcortical structures were considered for the analysis. Although neural activity signal was recorded from all lobes in both hemispheres, most of the recordings were obtained from the left temporal lobe (see an example of implantation scheme in Figure 1C). After preprocessing the data, we analyzed the Band Limited Power (BLP) at a given carrier frequency ($f_{carrier}$) in order to have specific spectral information. We bandpass filtered the iEEG signals within the narrow band [$f_{carrier}$-2, $f_{carrier}$+2 Hz] and considered a range $f_{carrier}$ = 1:4:130 Hz. In order to compute the envelope FC, we further computed the Hilbert transform (Figure 2). In order to study the global communication characteristics of the network states processing during the execution of a cognitive task, we contrasted two situations, namely: a pre-stimulus window of 500 ms before stimulus onset (pre-task condition), and a post-stimulus window of 500 ms following stimulus onset (task-condition). In order to characterize the organization of the network under both conditions, we used integration and segregation measures of global brain function (see Materials and Methods). Both measures characterize the broadness of functional communication across the different nodes of the underlying brain network.

The main results come from a comparison of the integration and segregation measures during the task and pre-task conditions. Here, we first focus on a single patient to demonstrate the main results (Figure

3). The neural integration significantly increases during cognitive processing (Figure 3A). Complementary to this measure, we observed a consistent decrease in segregation (as measured by the modularity measure, see Methods) during cognitive processing (Figure 3B). The greatest modulation appeared particularly in the gamma band (around 50 to 90 Hz). Paired *t-test* between task and pre-task conditions showed a significant modulation in all frequency bands ($p < 0.05$) for both measures.

Having found an increase in the integration consistently associated with a decrease in the segregation, we examined whether these changes could be explained by changes in the power spectrum. For this purpose, we calculated the power spectrum by Fast Fourier Transformations (FFT) methods. The results indicated that there were no iEEG power spectrum changes in any frequency induced by the task (Figure 3C) that could explain the increase of integration and decrease of modularity. Thus, the results suggest that the modulation of the integration and segregation during cognitive processing is positively associated with a global increase of broadcasting of communication, especially in the gamma band, by not modulating the level of oscillations but rather reorganizing probably the level of synchronization as suggested by the *Communication Through Coherence Theory* (CTC) (Fries, 2005; 2015). Furthermore, to check that this was not modulated by oscillations, we also computed the amplitude of the power spectrum at 60 Hz (with the maximal modulation of the integration measure) for each bipolar channel and for each condition. The strong overlap of the power across electrodes between pre-task and task conditions confirms that the level of oscillations are not responsible for the observed large changes in integration and segregation (Figure 3F).

Thus, we analyzed the level of global synchronization to test whether the increase of integration during cognitive processing is due to an increase of the coherence. To test this hypothesis, we used the Kuramoto Order Parameter (see Materials and Methods) to measure the mean level of synchronization of cortical activity under both conditions. We observed that, in fact, there is an increase of mean synchronization over a broad range of frequencies which is more conspicuous in the gamma band range (50 to 90 Hz) for the task condition (Figure 3D). This finding suggests a global functional network interaction linked to the inter-electrode communication.

Furthermore, we computed the Functional Connectivity between electrodes to see whether it behaves coherently with the other results. We calculated it through the instant amplitude envelopes of the given carrier frequencies ($f_{carrier}$= 1:4:130 Hz). The analysis revealed that the Functional Connectivity is enhanced during task performance, in particular in the gamma range (50 to 90 Hz) (Figure 3E).

Interestingly, both the integration and segregation modulations with task were consistently found in every patient despite the heterogeneity of the recording sites. Figures 4 and 5 plot for each single patient across conditions, the cognitive modulation of integration and segregation, respectively. As shown in those figures, the increase of integration and decrease of segregation relative to cognitive processing was

found at the individual level. It is clear that despite the heterogeneity of the recording sites, all of them show consistently the same pattern of modulation. Figure 6 plots the amplitude of the power spectrum at 60 Hz for each bipolar channel and for each patient. In all cases, the amplitude of the power spectrum across electrodes does not differ between pre-task and task conditions. Indeed, the majority of the electrodes (over 98.6%) do not show statistically significant differences in power modulation. Moreover, the minority of electrodes showing significant differences are only slightly modulated.

Discussion

We used intracranial EEG (iEEG) to record human neural activity from 12 epileptic patients while they were performing a picture-naming task in order to study how cognition modulates global functional network measurements, namely the integration and segregation. Across all patients, we found significant increases in integration and decreases in segregation during cognitive processing ($p<0.05$), especially in the gamma band (50-90 Hz). This was not driven by changes in the underlying level of oscillations given that the power spectra of task and pre-task conditions were indeed not significantly different. In contrast we found significantly higher level of synchronisation (as measured using the Kuramoto order parameter) and functional connectivity during the task, again particularly in the gamma band. Thus, the cognitive modulation of the broadness of communication across the entire extended network is putatively due to a rearrangement of the coherence level between the nodes, thus confirming the prediction of the CTC theory (Fries, 2005; 2015) but on a whole-brain level (Deco and Kringelbach, 2016).

Our results support the view of the brain as a complex system organized into large-scale networks. In order to support cognitive functions, the networks need to flexibly adjust their functional connectivity in order to integrate relevant information to support goal-directed behavior. Graph and information theoretical approaches have helped to characterize the global network connectivity in terms of *segregation* and *integration* (Tononi *et al.*, 1994; Fox & Friston, 2012; Deco *et* al., 2015). Here, segregation refers to the relative statistical independence of subsets of neurons or brain regions to compute information (Tononi *et al.*, 1994; Sporns, 2013); while integration is a complementary concept quantifying the level of broadcasting communication across the whole-brain (Sporns, 2013; Deco *et* al., 2015). In particular, we used a measure of integration based on the largest component present in the whole-brain connectivity matrix (Deco *et* al., 2015), while for the segregation we used the concept of modularity (Rubinov and Sporns, 2011).

Our findings are in line with previous neuroimaging studies finding increases of the integration across brain networks as evidenced by MEG during working memory processing (Kitzbichler *et al.*, 2011; Liang *et al.*, 2016), or by MRI during emotional and motivational stimulus processing (Kinnison *et al.*, 2012) and fMRI for selective attention (Elton and Gao, 2015). Moreover, our findings are also consistent with evidence supporting an increase of gamma-oscillations underlying language processing (Fukuda *et al*,. 2010; Wu *et al.*, 2011; Vidal *et al.*, 2012; see Jerbi *et al.*, 2009 for review)

More generally, our results provide support for the communication through coherence (CTC) mechanism for cognitive dynamics (Fries, 2005; 2015) at the whole brain network level. CTC hypothesis posits that the mechanism through which information is transmitted is by the synchronization of distinct neuronal populations, mainly in the gamma and beta-band (30-90 Hz) (Deco and Kringelbach, 2016).

It would be interesting to examine in future investigations how the integration and segregation measures are differently modulated under different cognitive load and as a function of the task were performed correctly or erroneously. An important future goal would be to go beyond global measures to determine specifically which brain areas or local networks shows the highest degree of task-driven effective connectivity and therefore are mostly involved in information processing. In this context, future studies would be greatly benefited from diffusion tensor imaging in twofold ways: to visualize and describe the precise location of the electrodes in the brain, as well as the basis of whole-brain models considering the connectivity and continuity of neural pathways in the patients.

There are certain methodological limitations due to the fact that iEEG in humans is always obtained from epileptic patients who, besides having epileptogenic neural activity, may have also differences in the structural connectivity (SC). On the other hand, the lack of whole-brain coverage with this technique means that we have to care when making assumptions of global network connectivity because of the restriction of the spatial coverage that can be simultaneously sampled.

In conclusion, we show that cognitive processing drives a global increase of integration and decrease of segregation, especially in the gamma band (50-90 Hz), related to broadcasting of communication.

Acknowledgements

The authors would like to thank all patients for their participation and the IMIM-Hospital del Mar Epilepsy Unit staff for their technical assistance in collecting the data. This work was supported by Gustavo Deco's ERC Advanced Grant: DYSTRUCTURE (n. 295129), from the European Union's Horizon 2020 research and innovation programme under grant agreement No. 720270 and by the Spanish Research Project PSI2013-42091-P. M.L.K. is supported by the ERC Consolidator Grant CAREGIVING (n. 615539) and the Center for Music in the Brain, funded by the Danish National Research Foundation (DNRF117)

References

Bassett, D. S., Wymbs, N. F., Porter, M. A., Mucha, P. J., Carlson, J. M., & Grafton, S. T. (2011). Dynamic reconfiguration of human brain networks during learning. *Proceedings of the National Academy of Sciences*,

108(18), 7641-7646.

Bertrand, J. A., Tremblay, J., Lassonde, M., Vannasing, P., Nguyen, D. K., Robert, M., ... & Lepore, F. (2014). Recognizing an object from the sum of its parts: An intracranial study on alpha rhythms. *Journal of cognitive neuroscience*, 26(8), 1797-1805.

Bola, M., & Sabel, B. A. (2015). Dynamic reorganization of brain functional networks during cognition. *Neuroimage*, 114, 398-413.

Boucher, O., D'Hondt, F., Tremblay, J., Lepore, F., Lassonde, M., Vannasing, P., ... & Nguyen, D. K. (2015). Spatiotemporal dynamics of affective picture processing revealed by intracranial high-gamma modulations. *Human brain mapping*, 36(1), 16-28.

Bressler, S. L., & Menon, V. (2010). Large-scale brain networks in cognition: emerging methods and principles. *Trends in cognitive sciences*, 14(6), 277-290.

Brookes MJ, Hale JR, Zumer JM, Stevenson CM, Francis ST, Barnes GR, Owen JP, Morris PG, Nagarajan SS (2011) Measuring functional connectivity using MEG: methodology and comparison with fcMRI. NeuroImage 56:1082-1104.

Burke, J. F., Zaghloul, K. A., Jacobs, J., Williams, R. B., Sperling, M. R., Sharan, A. D., & Kahana, M. J. (2013). Synchronous and asynchronous theta and gamma activity during episodic memory formation. *The Journal of Neuroscience*, 33(1), 292-304.

Cabral J, Luckhoo H, Woolrich M, Joensson M, Mohseni H, Baker A, Kringelbach ML, Deco G (2014) Exploring mechanisms of spontaneous functional connectivity in MEG: how delayed network interactions lead to structured amplitude envelopes of band-pass filtered oscillations. NeuroImage 90:423-435.

Chai, L. R., Mattar, M. G., Blank, I. A., Fedorenko, E., & Bassett, D. S. (2016). Functional Network Dynamics of the Language System. *Cerebral Cortex*.

Chan, A. M., Baker, J. M., Eskandar, E., Schomer, D., Ulbert, I., Marinkovic, K., ... & Halgren, E. (2011). First-pass selectivity for semantic categories in human anteroventral temporal lobe. *The Journal of Neuroscience*, 31(49), 18119-18129.

Deco, G., & Kringelbach, M. L. (2016). Metastability and coherence: extending the communication through coherence hypothesis using a whole-brain computational perspective. *Trends in neurosciences*, 39(3), 125-135.

Deco, G., Tononi, G., Boly, M., & Kringelbach, M. L. (2015). Rethinking segregation and integration: contributions of whole-brain modelling. *Nature Reviews Neuroscience*, 16(7), 430-439.

Ekman, M., Derrfuss, J., Tittgemeyer, M., & Fiebach, C. J. (2012). Predicting errors from reconfiguration patterns in human brain networks. *Proceedings of the National Academy of Sciences*, 109(41), 16714-16719.

Elton, A., & Gao, W. (2015). Task-related modulation of functional connectivity variability and its behavioral correlations. *Human brain mapping*, 36(8), 3260-3272.

Engel, A. K., Moll, C. K., Fried, I., & Ojemann, G. A. (2005). Invasive recordings from the human brain: clinical insights and beyond. *Nature Reviews Neuroscience*, 6(1), 35-47.

Fallani, F. D. V., Astolfi, L., Cincotti, F., Mattia, D., Tocci, A., Salinari, S., ... & Babiloni, F. (2008). Brain network analysis from high-resolution EEG recordings by the application of theoretical graph indexes. *IEEE Transactions on Neural Systems and Rehabilitation Engineering*, 16(5), 442-452.

Ferstl, E. C., Neumann, J., Bogler, C., & Von Cramon, D. Y. (2008). The extended language network: a meta-analysis of neuroimaging studies on text comprehension. *Human brain mapping*, 29(5), 581-593.

Fox, P. T., & Friston, K. J. (2012). Distributed processing; distributed functions?. *Neuroimage*, 61(2), 407-426.

Fries, P. (2005). A mechanism for cognitive dynamics: neuronal communication through neuronal coherence. *Trends in cognitive sciences*,9(10), 474-480.

Fries, P. (2015). Rhythms for cognition: communication through coherence.*Neuron*, 88(1), 220-235.

Fukuda, M., Rothermel, R., Juhász, C., Nishida, M., Sood, S., & Asano, E. (2010). Cortical gamma-oscillations modulated by listening and overt repetition of phonemes. *Neuroimage*, 49(3), 2735-2745.

Gaillard, R., Dehaene, S., Adam, C., Clémenceau, S., Hasboun, D., Baulac, M., ... & Naccache, L. (2009). Converging intracranial markers of conscious access.*PLoS Biol*, 7(3), e1000061.

Godwin, D., Barry, R. L., & Marois, R. (2015). Breakdown of the brain's functional network modularity with awareness. *Proceedings of the National Academy of Sciences*, 112(12), 3799-3804.

Greenberg, J. A., Burke, J. F., Haque, R., Kahana, M. J., & Zaghloul, K. A. (2015). Decreases in theta and increases in high frequency activity underlie associative memory encoding. *Neuroimage*, 114, 257-263.

Haque, R. U., Wittig, J. H., Damera, S. R., Inati, S. K., & Zaghloul, K. A. (2015). Cortical Low-Frequency Power and Progressive Phase Synchrony Precede Successful Memory Encoding. *The Journal of Neuroscience*, 35(40), 13577-13586.

Hamamé, C. M., Alario, F. X., Llorens, A., Liégeois-Chauvel, C., & Trébuchon-Da Fonseca, A. (2014). High frequency gamma activity in the left hippocampus predicts visual object naming performance. *Brain and language*, 135, 104-114.

Jerbi, K., Ossandon, T., Hamame , C. M., Senova, S., Dalal, S. S., Jung, J., et al. (2009). Task-related gamma-band dynamics from an intracerebral perspective: review and implications for surface EEG and MEG. Human Brain Mapping, 30(6), 1758e1771.

Kahana, M. J. (2006). The cognitive correlates of human brain oscillations. *The Journal of Neuroscience*, 26(6), 1669-1672.

Kinnison, J., Padmala, S., Choi, J. M., & Pessoa, L. (2012). Network analysis reveals increased integration during emotional and motivational processing.*The Journal of Neuroscience*, 32(24), 8361-8372.

Kitzbichler, M. G., Henson, R. N., Smith, M. L., Nathan, P. J., & Bullmore, E. T. (2011). Cognitive effort drives workspace configuration of human brain functional networks. *The Journal of Neuroscience*, 31(22), 8259-8270.

Kucewicz, M. T., Cimbalnik, J., Matsumoto, J. Y., Brinkmann, B. H., Bower, M. R., Vasoli, V., ... & Worrell, G. A. (2014). High frequency oscillations are associated with cognitive processing in human recognition memory. *Brain*, awu149.

Lachaux, J. P., Rudrauf, D., & Kahane, P. (2003). Intracranial EEG and human brain mapping. Journal of Physiology, 97(4e6), 613e628.

Lachaux, J. P., Axmacher, N., Mormann, F., Halgren, E., & Crone, N. E. (2012). High-frequency neural activity and human cognition: past, present and possible future of intracranial EEG research. *Progress in neurobiology*, 98(3), 279-301.

Liang, X., Zou, Q., He, Y., & Yang, Y. (2016). Topologically reorganized connectivity architecture of default-mode,

executive-control, and salience networks across working memory task loads. *Cerebral Cortex*, 26(4), 1501-1511.

Murray, R. J., Brosch, T., & Sander, D. (2014). The functional profile of the human amygdala in affective processing: insights from intracranial recordings.*Cortex*, 60, 10-33.

Müsch, K., Hamamé, C. M., Perrone-Bertolotti, M., Minotti, L., Kahane, P., Engel, A. K., ... & Schneider, T. R. (2014). Selective attention modulates high-frequency activity in the face-processing network. *Cortex*, 60, 34-51.

Newman, M. E. J. (2004). Fast algorithm for detecting community structure in networks. Physical Review E, 69, 066133.

Newman, M. E. (2006). Modularity and community structure in networks. *Proceedings of the national academy of sciences*, 103(23), 8577-8582.

Nir, Y., Mukamel, R., Dinstein, I., Privman, E., Harel, M., Fisch, L., ... & Kramer, U. (2008). Interhemispheric correlations of slow spontaneous neuronal fluctuations revealed in human sensory cortex. Nature neuroscience, 11(9), 1100-1108.

Ossandón, T., Vidal, J. R., Ciumas, C., Jerbi, K., Hamamé, C. M., Dalal, S. S., ... & Lachaux, J. P. (2012). Efficient "pop-out" visual search elicits sustained broadband gamma activity in the dorsal attention network. *The Journal of Neuroscience*, 32(10), 3414-3421.

Palva, S., Monto, S., & Palva, J. M. (2010). Graph properties of synchronized cortical networks during visual working memory maintenance. *Neuroimage*,49(4), 3257-3268.

Perez, O., Mukamel, R., Tankus, A., Rosenblatt, J. D., Yeshurun, Y., & Fried, I. (2015). Preconscious prediction of a driver's decision using intracranial recordings. *Journal of cognitive neuroscience*.

Price, C. J. (2000). The anatomy of language: contributions from functional neuroimaging. *Journal of anatomy*, 197(03), 335-359.

Rubinov, M., & Sporns, O. (2011). Weight-conserving characterization of complex functional brain networks. *Neuroimage*, 56(4), 2068-2079.

Sahin, N. T., Pinker, S., Cash, S. S., Schomer, D., & Halgren, E. (2009). Sequential processing of lexical, grammatical, and phonological information within Broca's area. *Science*, 326(5951), 445-449.

Serletis, D., Bulacio, J., Bingaman, W., Najm, I., & González-Martínez, J. (2014). The stereotactic approach for mapping epileptic networks: a prospective study of 200 patients: Clinical article. *Journal of neurosurgery*, 121(5), 1239-1246.

Sperling, M. R. (1997). Clinical challenges in invasive monitoring in epilepsy surgery. *Epilepsia* (Suppl.) 38, S6±S12.

Sporns, O. (2013). Network attributes for segregation and integration in the human brain. *Current opinion in neurobiology*, 23(2), 162-171.

Tononi, G., Sporns, O., & Edelman, G. M. (1994). A measure for brain complexity: relating functional segregation and integration in the nervous system. *Proceedings of the National Academy of Sciences*, 91(11), 5033-5037.

Valencia, M., Martinerie, J., Dupont, S., & Chavez, M. (2008). Dynamic small-world behavior in functional brain networks unveiled by an event-related networks approach. *Physical Review E*, 77(5), 050905.

Vatansever, D., Menon, D. K., Manktelow, A. E., Sahakian, B. J., & Stamatakis, E. A. (2015). Default mode dynamics for global functional integration. *The Journal of Neuroscience*, 35(46), 15254-15262.

Vidal, J. R., Freyermuth, S., Jerbi, K., Hamamé, C. M., Ossandon, T., Bertrand, O., ... & Lachaux, J. P. (2012). Long-distance amplitude correlations in the high gamma band reveal segregation and integration within the reading network.*The Journal of Neuroscience*, 32(19), 6421-6434.

Wang, N., Zhang, L., & Liu, G. (2015). EEG-based research on brain functional networks in cognition. *Bio-Medical Materials and Engineering*, 26(s1), S1107-S1114.

Wang, X., Zhen, Z., Song, Y., Huang, L., Kong, X., & Liu, J. (2016). The Hierarchical Structure of the Face Network Revealed by Its Functional Connectivity Pattern. *The Journal of Neuroscience*, 36(3), 890-900.

Wu, H. C., Nagasawa, T., Brown, E. C., Juhasz, C., Rothermel, R., Hoechstetter, K., ... & Asano, E. (2011). Gamma-oscillations modulated by picture naming and word reading: intracranial recording in epileptic patients.*Clinical Neurophysiology*, 122(10), 1929-1942.

Figures

Table 1. Demographics and clinical characteristics of each patient.

Patient	Gender	Age (years)	Epileptogenic zone laterality	Seizure onset zone	Implanted Regions	N° of electrodes implanted	N° unipolar channels	N° of bipolar channels for analysis
A	Male	38	Left	Mesial temporal & amygdala	L (F-T-I-P)	8	85	76
B	Male	21	Left	Anterior temporal	L (F-T-I-P-O) & R (F-T)	15	125	95
C	Male	44	Right	Anterior temporal	L (T) & R (F-T-P)	12	125	104
D	Male	44	Right	Temporo parietal	L (T) & R (F-T-I-P)	16	127	101
E	Female	43	Left	Anterior medial temporal	L (F-T-I-P-O)	11	127	112
F	Male	25	Right	Temporo parieto occipital	R (F-T-I-P-O)	14	127	105
G	Male	23	Left	Temporal	L (F-T-I-P)	13	125	102
H	Female	43	Left	Posterior Temporal	L (F-T-I-P)	14	125	103
I	Male	44	Left	Mesial Temporal	L (F-T-I-P)	12	123	105
J	Female	46	Left	Anterior medial temporal	L (F-T-I-P-O)	11	124	107
K	Male	43	Left	Mesial Temporal	L (F-T-P)	9	103	94
L	Male	23	Right	Anterior temporal	R (F-T-P)	15	125	96

R: Right; L: Left; F: Frontal; T: Temporal; P: Parietal; O: Occipital; I: Insula

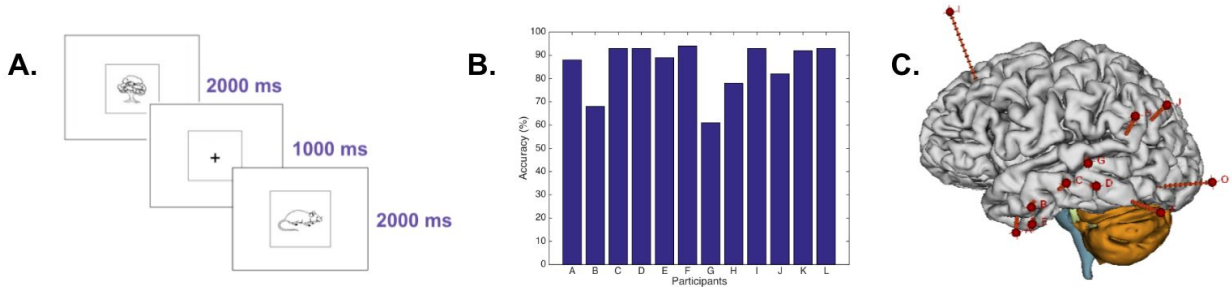

Figure 1. Paradigm, behavioral performance and implantation scheme. *A) Schematic example of the experimental paradigm. After an interval of 1000 ms for preparation, each target picture was presented and remained on the screen for 2000 ms. B) Picture naming accuracy for each patient. On average, patients achieved 85.3±11.0% accuracy on test items. C) Example of the intracerebral implantation scheme for iEEG recordings in patient E. Eleven electrodes were implanted in the left hemisphere.*

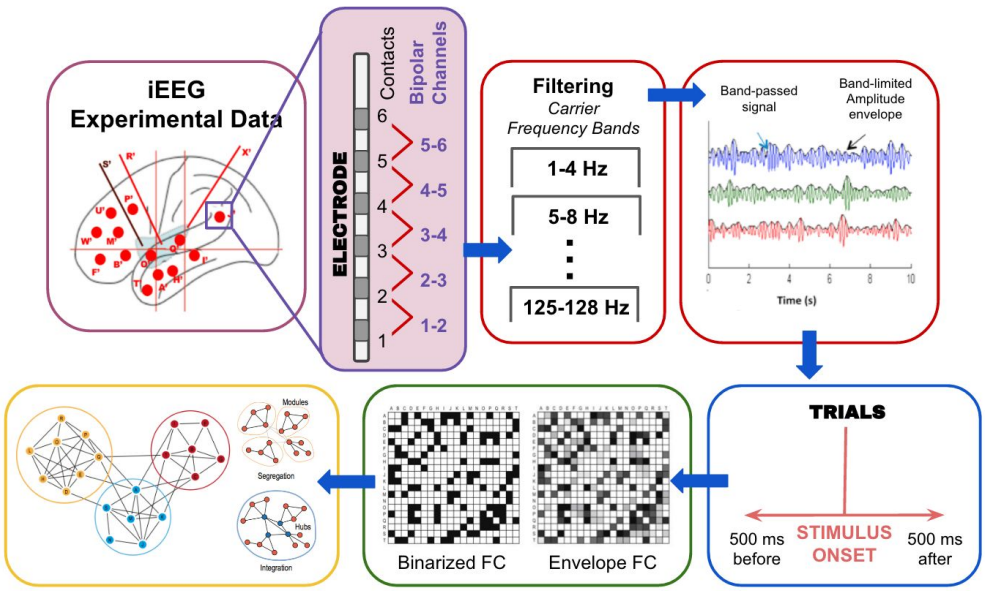

Figure 2. Data processing flow chart. *The iEEG data is recorded from 85 up to 127 unipolar channels on each patient. The bipolar montage is constituted offline by subtracting the neural activity recorded by neighbouring contacts within the same electrode array. The data is first bandpass filtered at 1 to 150 Hz, and further bandpass filtered into narrow frequency bands* $[f_{carrier}-2, f_{carrier}+2$ *Hz]* *(we consider here carrier frequencies* $f_{carrier}$ *= 1 to 130 Hz in steps of 4 Hz). By the Hilbert transform the corresponding amplitude envelopes are computed to further compute the envelope FC matrix. The continuous data is segmented into windows of -500 to 0 (pre-task condition) and 0 to 500 ms (task condition), around stimulus presentation. In order to characterize the organization of the network under both conditions, we used integration and segregation measures of global brain function.*

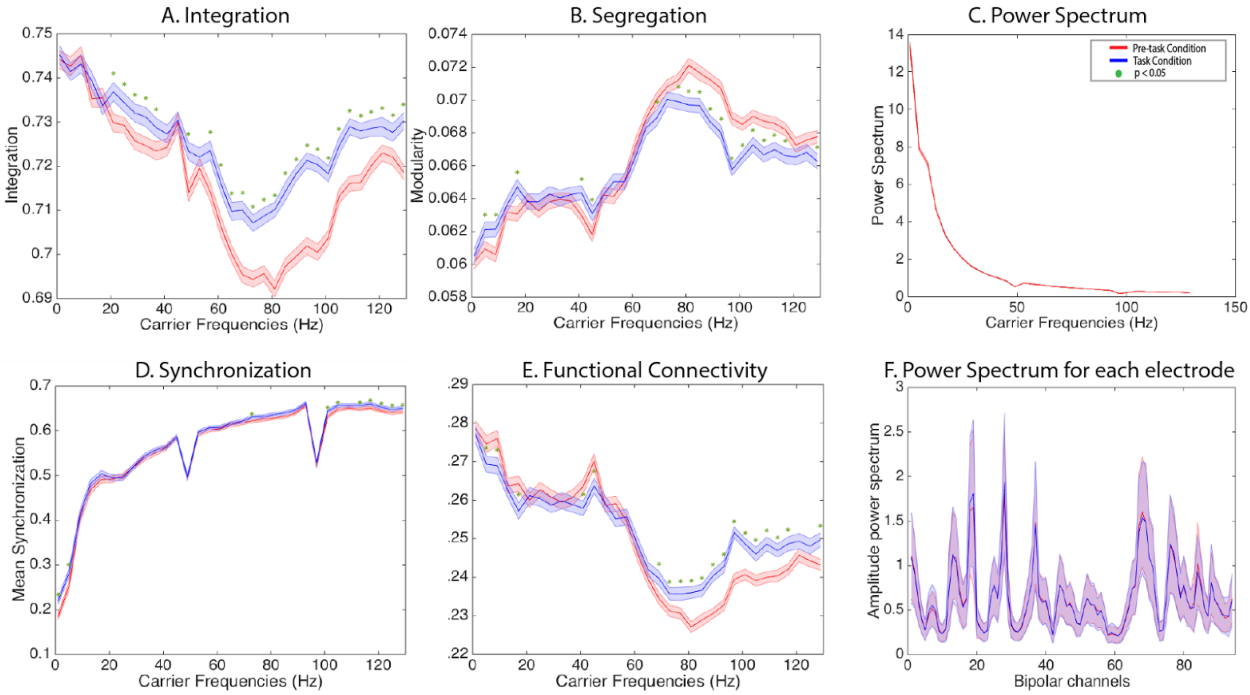

Figure 3. Results analysis patient K. *Panel A shows a significant increase in the integration during cognitive processing for all carrier frequencies, although it is clear that the greatest effect is observed in the gamma range* (50 to 90 Hz) (*p*<0.05). *The red line corresponds to pre-task condition, the blue line corresponds to task condition and green dots indicates an statistical significance of p*<0.05. *Complementary to the integration, panel B shows a decrease of the modularity in the same frequency range. Panel C shows that there are no iEEG power spectrum changes in any frequency induced by the task. This result indicates that the increase of integration and decrease of modularity could not be explain by changes in the power spectrum. Panel D shows an increase of mean synchronization over a broad range of frequencies which is more conspicuous in the gamma band range* (50 to 90 Hz) *for the task condition. Panel E shows that the functional connectivity behaves coherently with the other results as it increases as a function of the task load particularly in the gamma range* (50 to 90 Hz). *Panel F plots the amplitude of the power spectrum at 60 Hz for each bipolar channel and both pre-task and task conditions. There is no noticeable modulations across across single bipolar channels between pre-task and task conditions.*

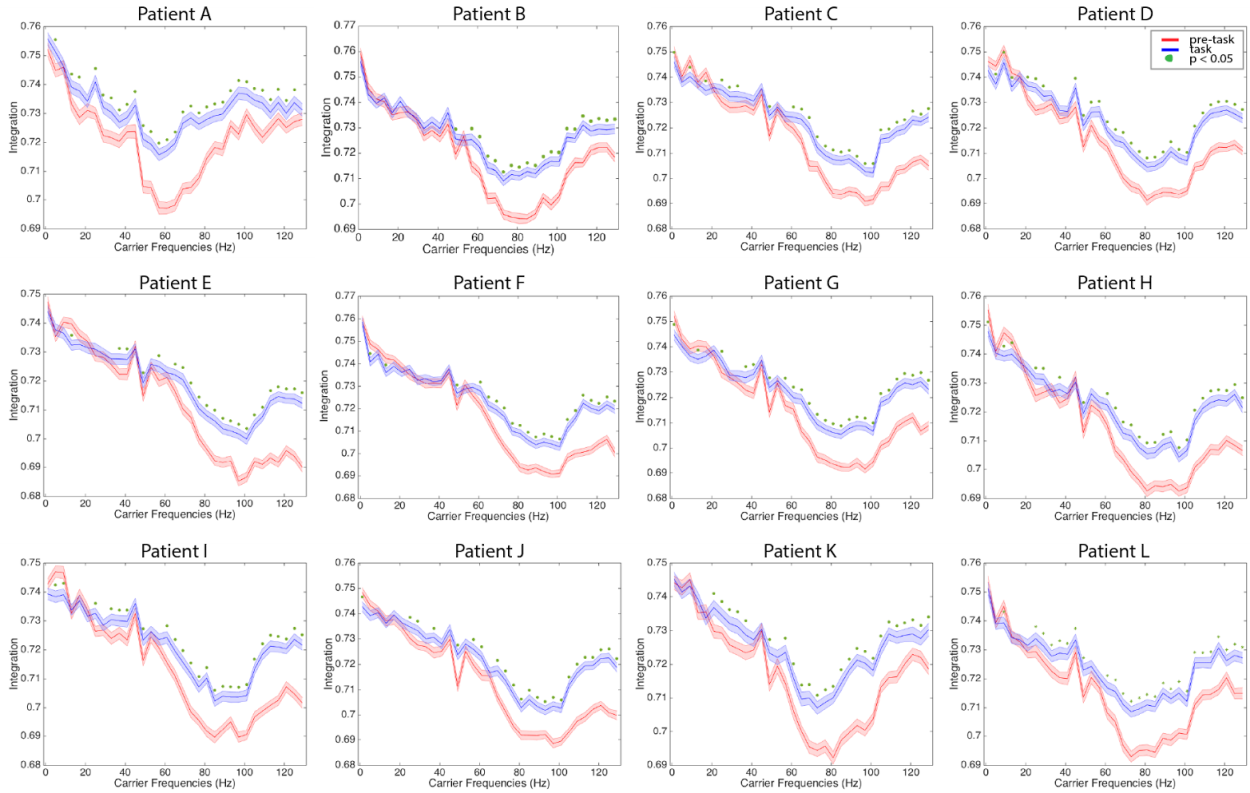

Figure 4. Integration measure results for each patient. *The panels shows the results for every single patient. As can be seen, despite the heterogeneity of the recording sites, all patients shows a significant increase of the integration related to cognitive processing (p<0.05). For all, the greatest effect was found in the gamma range. The red line corresponds to pre-task condition, the blue line corresponds to task condition and green dots indicates an statistical significance of p<0.05.*

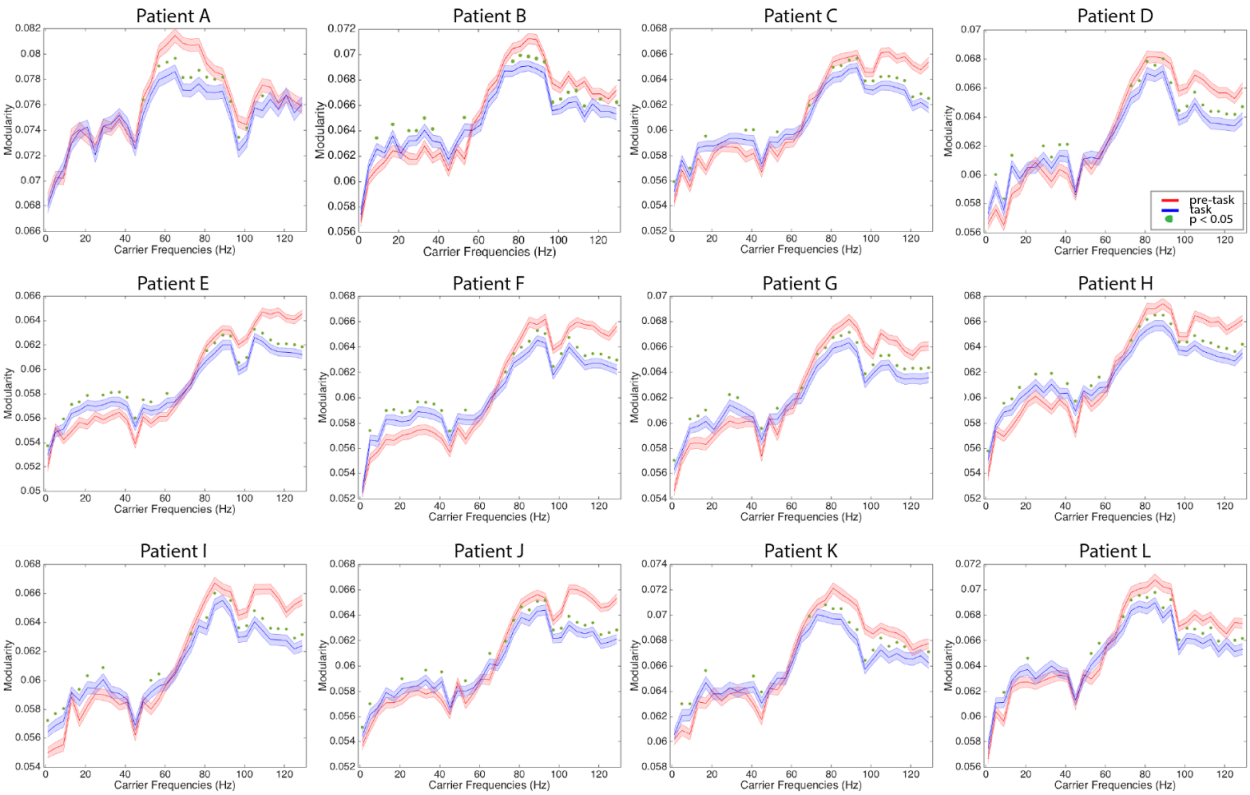

Figure 5. *Segregation measure results for each patient.* *The panels shows the results of segregation (measured by the modularity) during task and pre-task conditions. For all patients there is a significant decrease of the segregation during cognitive processing and the greatest effect can be seen in the gamma range (50 to 90 Hz) ($p<0.05$). The red line corresponds to pre-task condition, the blue line corresponds to task condition and green dots indicates an statistical significance of $p<0.05$.*

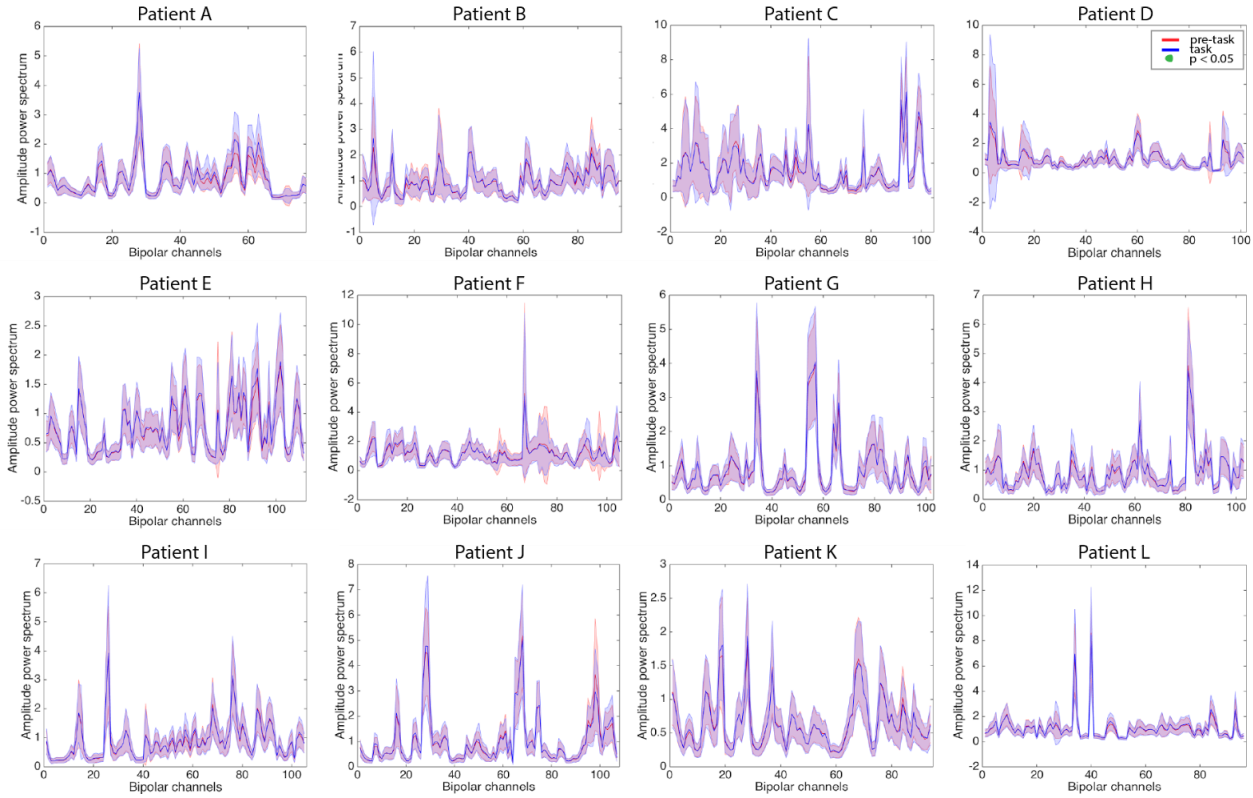

Figure 6. Amplitude of the Power Spectrum at 60 Hz across electrodes for each patient. *The panel shows the results of the amplitude of the power spectrum at 60 Hz for each bipolar channel and both pre-task and task conditions. For all patients there is no noticeable modulations across single bipolar channels between pre-task and task conditions. The red line corresponds to pre-task condition and the blue line corresponds to task condition.*